

Sign of hard X-ray pulsation from the gamma-ray binary system LS 5039

H. Yoneda,^{1,2,3} K. Makishima,^{2,1} T. Enoto,⁴ D. Khangulyan,⁵ T. Matsumoto,¹ and T. Takahashi^{2,1}

¹*Department of Physics, The University of Tokyo, 7-3-1 Hongo, Bunkyo, Tokyo 113-0033, Japan*

²*Kavli Institute for the Physics and Mathematics of the Universe (WPI),
University of Tokyo, Kashiwa, Chiba 277-8583, Japan*

³*RIKEN Nishina Center, 2-1 Hirosawa, Wako, Saitama 351-0198, Japan*

⁴*Extreme natural phenomena RIKEN Hakubi Research Team,*

Cluster for Pioneering Research, RIKEN, Hirosawa 2-1, Wako, Saitama, 351-0198, Japan

⁵*Department of Physics, Rikkyo University, 3-34-1 Nishi Ikebukuro, Toshima, Tokyo 171-8501, Japan*

(Dated: September 7, 2020)

To understand the nature of the brightest gamma-ray binary system LS 5039, hard X-ray data of the object, taken with the *Suzaku* and *NuSTAR* observatories in 2007 and 2016, respectively, were analyzed. The two data sets jointly gave tentative evidence for a hard X-ray periodicity, with a period of ~ 9 s and a period increase rate by $\sim 3 \times 10^{-10}$ s s⁻¹. Therefore, the compact object in LS 5039 is inferred to be a rotating neutron star, rather than a black hole. Furthermore, several lines of arguments suggest that this object has a magnetic field of several times $\sim 10^{10}$ T, two orders of magnitude higher than those of typical neutron stars. The object is hence suggested to be a magnetar, which would be the first to be found in a binary. The results also suggest that the highly efficient particle acceleration process, known to be operating in LS 5039, emerges through interactions between dense stellar winds from the massive primary star, and ultra-strong magnetic fields of the magnetar.

Introduction.— Gamma-ray binary systems are a recently established, yet rare, class of astronomical objects [1]. Their spectral energy distributions, peaked at above MeV energies, indicate extremely effective particle acceleration. Although most of the proposed scenarios claim that they contain a non-accreting neutron star (NS) or an accreting black hole [2], the answer has been unknown in most cases, let alone the detailed mechanism of their high-energy activity.

LS 5039 is the brightest gamma-ray binary system in the Galaxy, consisting of an O-type primary star with a mass of $23M_{\odot}$ and a compact secondary of unknown nature [3]. Its emission extends up to TeV energies, with a high bolometric luminosity of $\sim 1 \times 10^{29}$ W [1, 4]. It is suggested [5, 6] that particles are accelerated in this source with exceptionally high efficiency, e.g., up to tens of TeV in a few seconds.

Past observations of LS 5039 revealed remarkable reproductivity of the soft X-ray orbital light curve [7] and strong orbital-phase dependence in the gamma-ray spectrum [8, 9]. These results disfavor the accretion scenario, and suggest that LS 5039 harbors an NS. A plausible view [10, 11] was that it contains a rotation-powered pulsar, and its relativistic winds collide with the primary’s stellar winds and then shock acceleration takes place. This picture can explain the spec-

trum in the X-rays and GeV/TeV bands, but cannot reproduce the dominant component in MeV gamma-rays [4]. Therefore, the compact star in LS 5039 might not be an ordinary pulsar. It could alternatively be a magnetar, i.e., an NS with two orders of magnitude higher magnetic fields than typical pulsars, as suggested for another gamma-ray binary system LS I+61°303 based on its magnetar-like X-ray flare [12].

To confirm the presence of an NS (including a magnetar) in LS 5039, detection of periodical pulses would be crucial. Although such attempts using radio [13] and soft X-rays [14] have failed so far, hard X-rays will be a better probe since they are less affected by the primary’s stellar winds. We hence performed a pulsation search from LS 5039, for the first time in hard X-rays.

Observation.— LS 5039 was observed with the hard X-ray detector (HXD) [15] onboard *Suzaku* [16] from 2007 September 9 to 15 for a gross exposure of 497 ks (net 181 ks), covering about 1.5 orbital cycles [7]. The HXD was operated in the normal mode with a time resolution of 61 μ s. We utilize the events in 10–30 keV, with a total number of 8.2×10^4 , of which about 90% are background.

Nine years later, *NuSTAR* [17] observed LS 5039 from 2016 September 1 to 5 for a gross exposure of 346 ks (net 191 ks), or about one or-

bital cycle. We extracted 10–30 keV events from a circular region centered at the source with a radius of 30 arcsec. The total number of events is 1.2×10^4 of which 4% is background. The time resolution is 10 μ s after correcting for the clock drifts.

Method.— If the putative NS in LS 5039 has a mass of $\sim 1.4M_{\odot}$, its projected orbital radius should be ~ 50 light sec. Thus, individual pulses, suffering periodic changes by ~ 50 s in their arrival times, would be smeared out unless the pulse period is $P_{\text{NS}} \gg 50$ s. Although this problem could be avoided by correcting the photon arrival times for the NS’s binary motion, the orbital solutions currently available from optical observations [3, 18, 19] are not accurate enough for this purpose.

We thus search for pulsations, first without corrections for the NS’s orbital motion. Its line-of-sight velocity would cause the Doppler modulation up to

$$\Delta v/c \sim 50 \text{ (s)} \times 2\pi/P_{\text{orb}} = 1 \times 10^{-3} . \quad (1)$$

A simple way to mitigate this $\pm 0.1\%$ period change is to divide the whole data into many subsets, each with a duration of ΔT which is short enough to approximately satisfy

$$P_{\text{NS}}/\Delta T \gtrsim 1 \times 10^{-3} . \quad (2)$$

Then, the Fourier frequency resolution becomes no higher than Eq.(1). The power spectra thus calculated from individual subsets are merged incoherently into an averaged spectrum with improved statistics. Requiring each subset to include $\gtrsim 10$ source photons, we limit our search to $P_{\text{NS}} > 1$ s. Thus, we focus on slowly-rotating neutron stars (Supplemental Material (SM) §A [25]).

Results.— First, we Fourier-analysed the 10–30 keV HXD data over a frequency range of 10^{-2} –1.0 Hz, employing $\Delta T = 4096, 8192,$ and 16384 s, and obtained Figure 1 (a). The result for $\Delta T = 8192$ s reveals a clear peak at $P_{\text{NS}} = 8.96$ s, where the power reaches 3.79 above the average of 2.0. The post-trial probability of this peak was estimated as follows. As we used 55 data subsets when $\Delta T = 8192$ s, each Fourier component in Figure 1 (a) obeys a

χ^2 distribution with 110 d.o.f. (SM §B [25]) and the local chance probability of the 8.96 s peak becomes 4.5×10^{-8} . Because 8192 independent frequencies were tested, the chance probability considering look-elsewhere effects, becomes $\mathcal{P}_{\text{ch}} = 4.5 \times 10^{-8} \times 8192 = 3.7 \times 10^{-4}$. Finally considering a factor 3 which is the numbers of ΔT tested, we obtain $\mathcal{P}_{\text{ch}} = 1.1 \times 10^{-3}$. This estimation was also confirmed by a Monte-Carlo simulation. Thus, the 8.96 s periodicity has a confidence level close to 99.9%. The ratio $P_{\text{NS}}/\Delta T = 0.11\%$ is fully self-consistent within our framework; see Eq.(2). Furthermore, this periodicity is unlikely to be due to contamination from other sources (SM §C [25]).

The above result was further studied using Z^2 statistics [20], a test for weak periodic signals with unbinned likelihood evaluation. Using only the fundamental harmonic, we calculated Z^2 over $P_{\text{NS}} = 1$ –100 s, also from individual subsets of length ΔT , and incoherently stacked the results into a single Z^2 periodogram. We changed ΔT from 3000 s to 12000 s, with a step of 1000 s. Figure 1 (b-1) shows the case with $\Delta T = 5000$ s, where the periodicity appears clearly at $P_{\text{NS}} = 8.960 \pm 0.009$ s; the quoted error is dominated by the orbital Doppler shifts.

The significance of this Z^2 peak was evaluated with a Monte-Carlo method. In a single trial, we generated the entire subsets, each with the same photon counts and same observing windows as the actual data, but with no intrinsic periodicity. Each subset was Z^2 analyzed. The results were again stacked into a single periodogram covering $P_{\text{NS}} = 1$ –100 s, and the maximum Z^2 was registered. After 2×10^4 trials, we found 3 cases with the maximum Z^2 higher than in Figure 1 (b-1). This yields $\mathcal{P}_{\text{ch}} = 1.5 \times 10^{-4}$ for the observed peak, considering look-elsewhere effects over the 1–100 s range. Counting the 10 steps in ΔT , we finally obtain $\mathcal{P}_{\text{ch}} = 1.5 \times 10^{-3}$ in agreement with the Fourier analysis.

Similarly, we analyzed the 10–30 keV *NuSTAR* data of LS 5039. First, we performed the same Fourier analysis, using $\Delta T = 4096, 8192,$ and 16384 s, but found no significant peaks in the averaged power spectra. To search for weaker pulsations, the data were then analyzed with the Z^2

statistics. We again used only the fundamental harmonic, and limited the search range to $P_{\text{NS}} = 7\text{--}11$ s, which accommodates period changes at a rate of $|\dot{P}_{\text{NS}}| < 7.0 \times 10^{-9}$ s s $^{-1}$, from the value indicated by *Suzaku*. We again changed ΔT from 3000 s to 12000 s, with a step of 1000 s. When $\Delta T = 10000$ s, the *NuSTAR* data yielded an obvious peak at $P_{\text{NS}} = 9.046 \pm 0.009$ s, as in Figure 1 (b-2). Additionally, the Z^2 value took the maximum at 9.046 s regardless of ΔT .

Again, the significance of this Z^2 peak was Monte-Carlo evaluated. After 2×10^4 trials, we found 62 cases with Z^2 higher than in Figure 1 (b-2). This yields $\mathcal{P}_{\text{ch}} = 3.1 \times 10^{-3}$ for this peak, considering look-elsewhere effects for the limited period search range of 7–11 s. Including the trials of ΔT , we obtain $\mathcal{P}_{\text{ch}} \lesssim 3.1 \times 10^{-2}$.

The two observations 9 years apart by the two satellites thus gave evidence for the ~ 9 s hard X-ray pulsation. Therefore, the compact object in LS 5039 is inferred to be an NS with a spin period of $P_{\text{NS}} \sim 9$ s, and its derivative of $\dot{P}_{\text{NS}} \sim 3 \times 10^{-10}$ s s $^{-1}$.

Finally, to confirm that the pulsed emission really comes from the compact object in LS 5039, we repeated the Z^2 analysis separately using the entire *Suzaku* and *NuSTAR* data sets, subdividing neither of them, but correcting the photon arrival times for the orbital motion. The orbital period was fixed at the optical value of $P_{\text{orb}} = 3.90608$ days [18]. We first scanned the orbital parameters over the ranges given in Table I. After finding a Z^2 maximum (separately for the two data sets), finer search steps were employed. We used the harmonics up to $m = 4$ to describe the pulse-profile details.

The *Suzaku* data yielded the orbital parameters as shown in Table I. They are consistent with the optical information. As the *NuSTAR* data gave several orbital solutions with comparable significance, Table I lists the one that is closest to the *Suzaku* solution (SM §E [25]). The *Suzaku* and *NuSTAR* pulse profiles, derived with the respective orbital solutions, are shown in Figure 2; they exhibit similar three peaks with separations of ~ 0.25 pulse phases.

Figure 3 shows the Z^2 periodograms after applying the orbital solutions in Table I. Both the

Suzaku and *NuSTAR* data show clear peaks, with pre-trial probabilities of 1.7×10^{-11} and 7.3×10^{-11} , respectively. Considering look-elsewhere effects, these yield $\mathcal{P}_{\text{ch}} = 1.2 \times 10^{-2}$ (*Suzaku*) and $\mathcal{P}_{\text{ch}} = 7.0 \times 10^{-2}$ (*NuSTAR*), since the number of independent trials in the parameter search was Monte-Carlo estimated as 7.2×10^8 and 9.6×10^8 , respectively. For further examination, we scanned P_{orb} , to find that the pulse significance becomes maximum at $P_{\text{orb}} = 3.90 \pm 0.05$ (*Suzaku*) and 3.94 ± 0.08 days (*NuSTAR*) in a good agreement with the reported value.

Although we have thus obtained signs of pulsation from LS 5039, we are still left with several problems. (1) The orbital solutions from the two data disagree on some parameters beyond their statistical errors. (2) The orbital corrections did not increase the pulse significance as large as expected. (3) After background subtraction, the two data give rather different pulse fractions (Figure 2), 0.68 ± 0.14 (*Suzaku*) and 0.135 ± 0.043 (*NuSTAR*). The 10–30 keV fluxes were also different from each other, $(10.7 \pm 1.2) \times 10^{-12}$ erg cm $^{-2}$ s $^{-1}$ (*Suzaku*) and $(8.26 \pm 0.10) \times 10^{-12}$ erg cm $^{-2}$ s $^{-1}$ (*NuSTAR*).

To find clues to these issues, we subdivided the *Suzaku* and *NuSTAR* data into several segments of similar lengths, and folded each with the orbital solution. Although these segments reproduced the pulse profile globally, its fine structures varied (SM §F [25]). Thus, the pulses could suffer from some modulation besides the orbital motion, which may have biased the orbital parameters beyond statistical errors.

We also analyzed the 3–10 keV *NuSTAR* data using the parameters in Table I, but found no periodic signals at the period. The upper-limit pulse fraction is 2.8% (99% confidence level, SM §G [25]).

Discussion.— We have obtained evidence for a ~ 9 s pulsation from LS 5039. Moreover, the mass of this pulse emitter is constrained as $1.23\text{--}2.35 M_{\odot}$ (SM §A [25]). We therefore infer that LS 5039 harbors an NS; this would settle the controversy as to the compact object in this system.

Our results also provide clues to the energy

source that powers the remarkable non-thermal processes of LS 5039. Generally, we can think of four candidates; rotational energy of the NS, stellar winds from the massive star, gravitational energy due to mass accretion, and magnetic energy of the NS. From the detected P_{NS} and its derivative \dot{P}_{NS} , the first one is excluded immediately, because the spindown energy loss of the NS, $L_{\text{SD}} = (2\pi)^2 I \dot{P}_{\text{NS}} / P_{\text{NS}}^3 \sim 10^{27} \text{ W}$ with I the NS moment of inertia, is much below the observed luminosity of $\sim 10^{29} \text{ W}$. The same applies to the second candidate, because the power available in this case is $< 10^{25} \text{ W}$ (SM §H [25]). The third candidate is also excluded, because neither the MeV-peaked spectrum nor the largely positive \dot{P}_{NS} of LS 5039 is observed from accreting pulsars. The good reproducibility of the soft X-ray orbital light curve also disfavors the accretion scenario [7].

Hence the sole option is left: dissipation of the NS's magnetic energy, of which the available output is given as

$$L_{\text{BF}} = \frac{B_{\text{NS}}^2 R_{\text{NS}}^3}{6\tau} \sim 10^{30} \left(\frac{B_{\text{NS}}}{10^{11} \text{ T}} \right)^2 \left(\frac{\tau}{500 \text{ yr}} \right)^{-1} \text{ W}, \quad (3)$$

where $R_{\text{NS}} \approx 10 \text{ km}$, B_{NS} , and $\tau = \frac{1}{2} P_{\text{NS}} / \dot{P}_{\text{NS}} \sim 500 \text{ yr}$ denote the NS's radius, surface magnetic field, and the characteristic age, respectively. Then, the need for $L_{\text{BF}} > 10^{29} \text{ W}$ is satisfied if $B_{\text{NS}} \gtrsim 3 \times 10^{10} \text{ T}$. This B_{NS} corresponds to those of magnetars, whose radiation is powered by their magnetic energies. This scenario is reinforced by the detected $P_{\text{NS}} \sim 9 \text{ s}$, which is typical of magnetars [21]. Additionally, the sporadic variations in the pulse properties, suggested by the present data, are also observed from magnetars [22, 23].

The magnetar scenario can also explain the absence of accretion in LS 5039. In these binaries, the ram pressure of the primary's stellar winds is balanced by the NS's magnetic pressure, at a

radius

$$R_{\text{A}} = \frac{R_{\text{NS}} (B_{\text{NS}} a_{\text{x}})^{1/3}}{(2\dot{M}_{\text{w}} v_{\text{w}})^{1/6}} \sim 2 \times 10^8 \left(\frac{B_{\text{NS}}}{10^{11} \text{ T}} \right)^{1/3} \text{ m}, \quad (4)$$

where $a_{\text{x}} \sim 50 \text{ light-sec}$ is the binary separation, $\dot{M}_{\text{w}} = 10^{-6} M_{\odot} \text{ yr}^{-1}$ is a typical wind mass-loss rate of O stars, and $v_{\text{w}} = 2000 \text{ km s}^{-1}$ is the typical wind velocity. For $B_{\text{NS}} \gtrsim 2 \times 10^{10} \text{ T}$, this R_{A} exceeds the Bondi-Hoyle capture radius $R_{\text{B}} \sim 1 \times 10^8 \text{ m}$: the strong magnetic pressure suppresses the gravitational wind capture.

As already suggested for another system [12], we thus propose that LS 5039 harbors a magnetar, with $B_{\text{NS}} \sim$ several times 10^{10} T . For reference, $B_{\text{NS}} \sim 10^{11} \text{ T}$ is also derived assuming the object to spin down via magnetic dipole radiation, but this should be taken as an upper limit since the spindown would be accelerated by interactions with the stellar winds.

Compared to LS 5039, isolated magnetars are less luminous ($\sim 10^{28} \text{ W}$), and lack the strong MeV component [24]. These differences may be attributed to the uniqueness of LS 5039 that it is immersed in the dense stellar winds. We hence suggest that interactions of the strong magnetic field with the stellar winds are essential, both in generating the distinctive non-thermal emission and enhancing its magnetic energy dissipation to afford a higher luminosity. A plausible scenario is that the stellar wind pressure rearranges the magnetar's magnetosphere and its magnetic energy is converted efficiently into radiation via, e.g., magnetic reconnection. TeV electrons would be produced efficiently in the reconnection region. Possibly, the MeV emission is also produced therein, via synchrotron radiation in the strong magnetic fields.

In closing, we found a periodicity around 9 s from the *Suzaku* hard X-ray data with a post-trial probability of 1.1×10^{-3} . Moreover, the *NuSTAR* data gave tentative evidence of the 9 s pulsation. These data jointly suggest $\dot{P}_{\text{NS}} \sim 3 \times 10^{-10} \text{ s s}^{-1}$, although further confirmation of these values is needed since the *NuSTAR* detection is not significant by itself. With this

reservation, our result is thought to have the three-fold significance. (1) It casts light on a novel scenario for the highly efficient acceleration mechanism in astrophysics. (2) The NS in LS 5039, the first magnetar candidate found in a binary, will provide clues to the birth and evolution of magnetars. (3) Refining the mass constraint through future observations, we may possibly tell whether the mass range of magnetars is different from that of ordinary NSs.

H.Y. acknowledges the support of the Advanced Leading Graduate Course for Photon Science (ALPS). We acknowledge support from JSPS KAKENHI grant numbers 16H02170, 16H02198, 17J04145, 18H01246, 18H05463, 18H03722, 18K03694, and 20H00153.

-
- [1] G. Dubus, *Astronomy and Astrophysics Review* **21**, 64 (2013).
 - [2] I. Mirabel, *Science* **335**, 6065 (2012).
 - [3] J. Casares *et al.*, *Mon. Not. R. Astr. Soc.* **364**, 899 (2005).
 - [4] W. Collmar and S. Zhang, *Astron. & Astrophys.* **565**, A38 (2014).
 - [5] T. Takahashi *et al.*, *Astrophys. J.* **697**, 592 (2009).
 - [6] D. Khangulyan, F. Aharonian, and V. Bosch-Ramon, *Mon. Not. R. Astr. Soc.* **383**, 467(2008).
 - [7] T. Kishishita *et al.*, *Astrophys. J.* **697**, L1 (2009).
 - [8] F. Aharonian *et al.*, *Astron. & Astrophys.* **460**, 743 (2006).
 - [9] A. A. Abdo *et al.*, *Astrophys. J.* **706**, L56 (2009).
 - [10] G. Dubus, A. Lamberts, and S. Fromang, *Astron. & Astrophys.* **581**, A27 (2015).
 - [11] J. Takata *et al.*, *Astrophys. J.* **790**, 18 (2014).
 - [12] D. F. Torres *et al.*, *Astrophys. J.* **744**, 106 (2012).
 - [13] M. Virginia McSwain *et al.*, *Astrophys. J.* **738**, 105 (2011).
 - [14] N. Rea *et al.*, *Mon. Not. R. Astr. Soc.* **416**, 1514 (2011).
 - [15] T. Takahashi *et al.*, *Publications of the Astronomical Society of Japan* **59**, S35 (2007).
 - [16] K. Mitsuda *et al.*, *Publications of the Astronomical Society of Japan* **59**, S1 (2007).
 - [17] F. A. Harrison *et al.*, *Astrophys. J.* **770**, 103 (2013).
 - [18] C. Aragona *et al.*, *Astrophys. J.* **698**, 514 (2009).
 - [19] G. E. Sarty *et al.*, *Mon. Not. R. Astr. Soc.* **411**, 1293 (2011).
 - [20] O. C. de Jager, B. C. Raubenheimer, and J. W. H. Swanepoel, *Astron. & Astrophys.* **221**,180 (1989).
 - [21] T. Enoto *et al.*, *Astrophys. J. Letters* **722**, L162 (2010).
 - [22] P. M. Woods *et al.*, *Astrophys. J.* **605**, 378 (2004).
 - [23] K. Makishima *et al.*, *Physical Review Letters* **112**, 171102 (2014).
 - [24] T. Enoto *et al.*, *Publications of the Astronomical Society of Japan* **63**, 387 (2011).
 - [25] See Supplemental Material [url], which includes Refs. [26–30].
 - [26] J. Moldón *et al.*, *Astron. & Astrophys.* **543**, A26 (2012).
 - [27] J. J. Condon *et al.*, *The Astronomical Journal* **115**, 1693 (1998).
 - [28] G. Hobbs *et al.*, *Mon. Not. R. Astr. Soc.* **353**, 1311 (2004).
 - [29] M. P. Muno *et al.*, *Astrophys. J.* **680**, 639 (2008).
 - [30] P. Reig *et al.*, *Astron. & Astrophys.* **405**, 285 (2003).

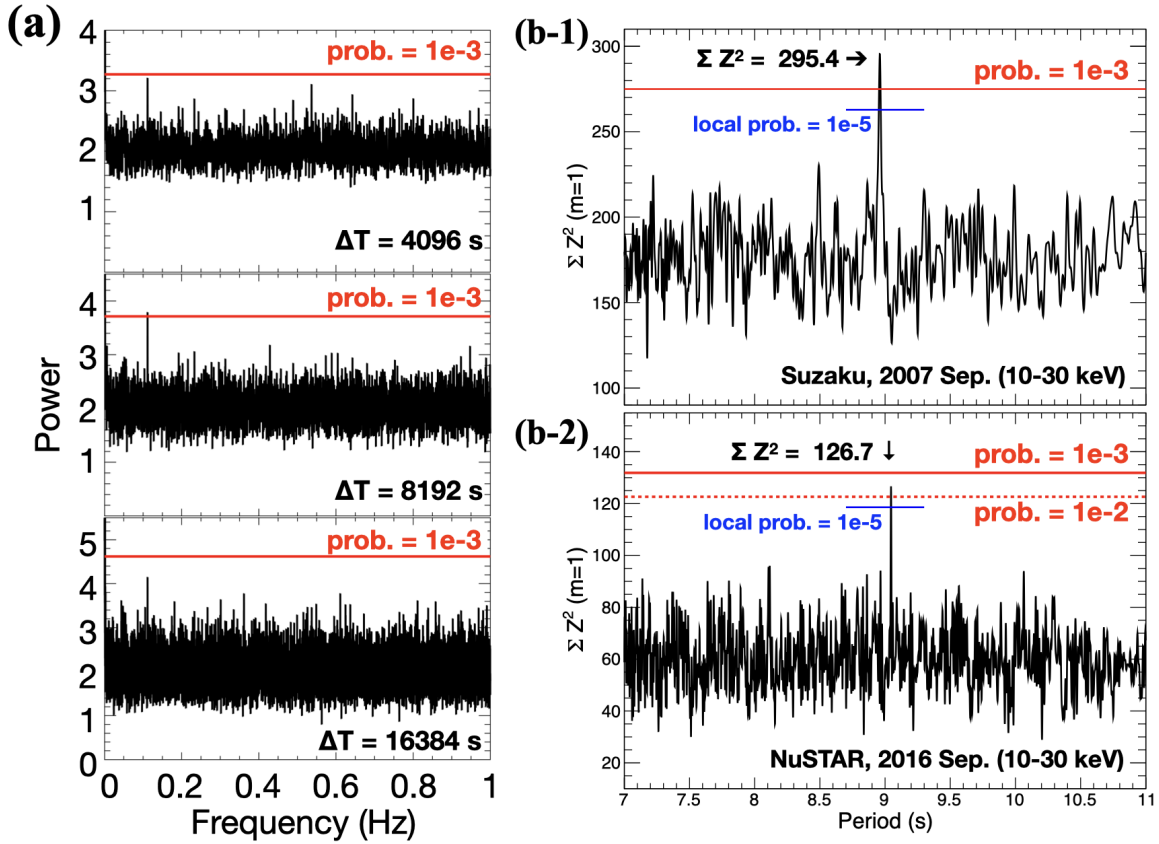


FIG. 1. Evidence of the pulsation from LS 5039. (a) Fourier analysis of the 10–30 keV *Suzaku* data, where red lines indicate signal strengths that arise with a post-trial probability of 1.0×10^{-3} when considering the look-elsewhere effect. The data are divided into subsets with $\Delta T = 4,096$, 8,192, and 16,384 s, and the power spectra from individual subsets are averaged. (b) Z^2 periodograms in 10–30 keV, shown for $P_{NS} = 7\text{--}11$ s. Panel (b-1) shows the *Suzaku* result (though the search was conducted over 1–100 s), averaged over 86 subsets with $\Delta T = 5,000$ s, and panel (b-2) that of *NuSTAR* from 30 subsets with $\Delta T = 10,000$ s.

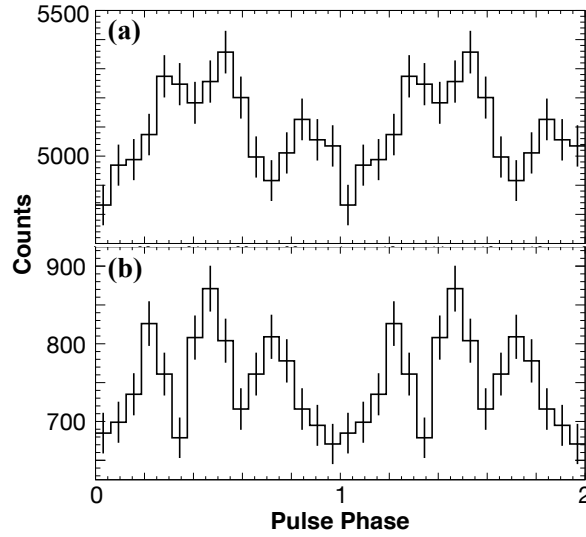


FIG. 2. The 10–30 keV folded pulse profiles from *Suzaku* (panel a) and *NuSTAR* (panel b), obtained using the best-estimated orbital parameters and optimum P_{NS} of the respective observations (Table I).

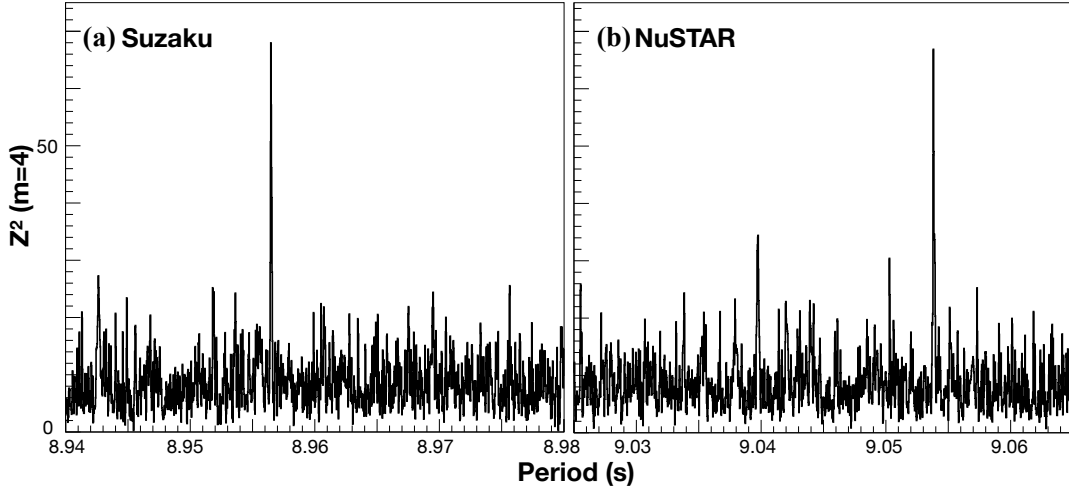


FIG. 3. Z^2 periodograms calculated coherently using the entire data of *Suzaku* (panel a) and *NuSTAR* (panel b), after the orbital-motion corrections using the best-fit parameters in Table I. Here up to the 4th harmonics are incorporated.

TABLE I. The search ranges of the orbital parameters and the best-fit results, obtained from *Suzaku*/*NuSTAR* observations. Errors of the best-fit values refer to 90% confidence limits.

parameter	search range		best-fitting value		optical results	
	min	max	<i>Suzaku</i>	<i>NuSTAR</i>	[18]	[19]
$a_x \sin \theta$ [light sec.]	30.0	67.375	$53.05^{+0.70}_{-0.55}$	$48.1^{+0.4}_{-0.4}$	-	-
e	0.16	0.39	$0.278^{+0.014}_{-0.023}$	$0.306^{+0.015}_{-0.013}$	0.337 ± 0.036	0.24 ± 0.08
ω [deg.]	45	65	$54.6^{+5.1}_{-3.3}$	$56.8^{+2.3}_{-3.1}$	56.0 ± 5.8	57.3 ± 21.8
τ_0 (<i>Suzaku</i>)*	-0.05	0.06875	$0.067^{+0.009}_{-0.012}$	-	-0.022 ± 0.017	0.030 ± 0.07
τ_0 (<i>NuSTAR</i>)*	0.5	0.74875	-	$0.7285^{+0.0078}_{-0.0058}$	0.546 ± 0.034	0.615 ± 0.33
P_{NS} [s] (<i>Suzaku</i>)	8.94	8.98	8.95648(4)	-	-	-
P_{NS} [s] (<i>NuSTAR</i>)	9.025	9.065	-	9.05381(3)	-	-
$Z^2(m=4)$	-	-	67.97	66.87	-	-

*: The orbital phase at the time of the initial event in the data. The time of the initial event of *Suzaku* and *NuSTAR* is 54352.7163 and 57632.0952 (MJD TT) respectively.